UDC 621.65

RESEARCH OF THE TORQUE-FLOW PUMP OPERATING PROCESS WITH A NON-CYCLIC IMPELLER IN THE OPERATING RANGE

Kondus Vladyslav Yuriyovych
Candidate of Technical Sciences, Associate Professor
Sumy State University, Sumy, Ukraine
ORCID: 0000-0003-3116-7455
v.kondus@pgm.sumdu.edu.ua

Krugliak Andrii Andriyovych
Ph.D. student
Sumy State University, Sumy, Ukraine
ORCID: 0009-0006-0279-9145
a.kruhlyak@pgm.sumdu.edu.ua

Baga Vadym Mykolayovych
Candidate of Technical Sciences, Associate Professor
Sumy State University, Sumy, Ukraine
ORCID: 0000-0003-0258-695X
v.baga@kttf.sumdu.edu.ua

Dumanchuk Mykhailo Yuriiuvych
Candidate of Technical Sciences, Associate Professor
Sumy National Agrarian University, Sumy, Ukraine
ORCID: 0000-0003-3559-4729
mykhailo.dumanchuk@snau.edu.ua

Torque-flow (TFP) pumps are widely used in various industries for pumping contaminated, fibrous or gas-containing liquids due to their simple design, reliability and low risk of clogging, despite the limitations of efficiency and head. The main disadvantages of torque-flow pumps are low energy efficiency (pump efficiency η=0.38-0.58) and the possibility of clogging of their flow part by the pumped product. This problem can be solved by ensuring the self-cleaning effect of the torque-flow pump by designing the impeller with a non-cyclic arrangement of blades, which will ensure a pulsating nature of the pressure in its inter-blade channels. The aim of the study was to establish the characteristics of a pump with non-cyclic arranged blades and compare the results obtained with the characteristics of a similar pump with evenly arranged blades. To conduct a numerical research in the ICEM CFD software package, unstructured computational meshes of the stator element (housing) and the rotor element (impeller) were created. The pump operating process was simulated in a stationary setting using the Ansys CFX software package, and the k-ε turbulence model in a stationary setting was used, water at a temperature of 25°C was used as the operating medium. According to the results of the study, it was found that when using an impeller with a non-cyclic arrangement of blades (with no blades), there is an increase in the relative velocity near the operating side of the blade in the expanded inter-blade channel, an uneven distribution of relative velocity at the entrance to the wheel simultaneously with the appearance of a flow separation zone in the inter-blade channels, which leads to increased losses, reduced pressure and, accordingly, pump efficiency. At the same time, the above allows us to state that according to Bernoulli's law, there is some increased pressure in the expanded impeller channels with a non-cyclic arrangement of blades in the reduced speed zones. This increased pressure creates the prerequisites for unstable relative motion of the operating fluid compared to using a standard impeller. In turn, this mechanism can be used as a self-cleaning mechanism for torque-flow pumps.

Key words: *UN SDGs, vibration reliability, life cycle cost, energy efficiency, durability, self-cleaning effect in pumps.*

DOI https://doi.org/10.32782/msnau.2024.4.1

Introduction. Nowadays, torque-flow pumps (TFP) are widely used in various branches of ukrainian and global industry, as well as in the national economy. These pumps are designed for pumping contaminated liquids, liquids with solid and fibrous impurities, as well as liquids with gaseous components (Panchenko et al., 2021).

The effectiveness of their use for such tasks is determined by their design and operational characteristics (Gao, et al., 2014):

− simplicity of design (for example, the absence of front seals and the simple shape of the flowing part);

− the special location of the impeller and the presence of a free chamber allow a significant part of the liquid to pass without contact with the wheel;

− low probability of clogging of the pump due to clogging of the flow part.

The combination of these factors ensures high wear resistance and reliability of the pumps (Quan, et al., 2019). In addition, the possibility of quick maintenance and repair increases the efficiency of their use in various fields (Antonenko, et al., 2021). This largely compensates for their economic disadvantages. At the same time, the main disadvantages of TFP pumps are their low efficiency (up to 58%) and a limited height of liquid rise (up to 100 m) compared to centrifugal analogues (Gusak, et al., 2017).

Torque-flow pumps are actively used today in various industries (Krishtop, et al., 2015), in particular in the food and chemical industries. They are also used in communal and agricultural industries for pumping fecal, soil and wastewater, as well as silt.

In the transport sector, these pumps are used to move fruit, fish, juices, suspensions, syrups and other substances such as wood pulp, waste paper, polymers and gaseous liquids (Kotenko, et al., 2014).

In addition, they have promising applications in energy (in particular, thermal energy), metallurgy, mining, as well as in the oil and coal industries (Kondus, et al., 2018).

At the same time, torque-flow pumps are a relatively new type of pumping equipment, which is characterized by ease of use and provides high reliability, durability and economic efficiency when operating with two- or more faze hydraulic mixtures. They also effectively cope with the transportation of various solid substances and products (Kumar, et al., 2023; Kondus & Kotenko, 2017).

Analysis of the components of the life cycle of pumping equipment and the main trends in the development of the pump market indicate the advantages of torque-flow pumps (TFP) (Krishtop, et al., 2014) when pumping liquids with a high content of abrasive particles, suspensions with a large content of solids and fibrous impurities, liquids with increased density, as well as liquids with a high air or gas content (Rogovyi, et al., 2022; Dehnavi, et al., 2023). They also effectively handle shear-sensitive liquids and liquids with fragile components, ensuring smooth and continuous transport of fibrous slurries. (Jung, et al., 2023).

Despite their numerous advantages, torque-flow pumps (TFP) also have disadvantages, the main of which is low efficiency (the efficiency of the pump is η=0.38-0.58) (Dehghan, et al., 2024). However, despite this drawback, the use of torque-flow pumps still provides a significant economic effect, thanks to their reliability, durability and efficiency when operating with various liquids.

It should be noted that in research (Kondus, et al., 2024) the authors proved the perspective of using impellers with a non-cyclic arrangement of blades for the purpose of forming a self-cleaning mechanism of torque-flow pumps.

Materials and Methods. Taking into account the above data, the purpose of the study is to establish the characteristics of a pump with unevenly spaced blades and to compare the obtained results with the characteristics of a similar pump with evenly spaced blades in the area of possible use of the pump, namely in the range of $Q=0.6–1.2Q_{BEP}$. Achieving the set goal contributes to the achievement of "industry, innovation and infrastructure" (SDG9) and "clean water and proper sanitation" (SDG6).

At the same time, the torque-flow pump TFP 125-60 was chosen as the research object with parameters: flow rate Q – 125 m^3/h, head – 60 m, rotation frequency – 1500 rpm, efficiency – 40%.

To achieve this goal, the following tasks are set:

− development of designs of impellers with the specified arrangement of blades (8 blades for uniform and 6 blades for uneven arrangement);

− creation of solid-state models of the operating environment for the stator part (free chamber) and the rotor part (impeller);

− assignment of initial conditions for conducting a numerical research in the ANSYS CFX Pre environment;

− carrying out a numerical research using the Solver software package;

− analysis of the obtained pump parameters for the studied operating range in CFX-Post.

The design of the blades of the impeller (Fig. 1) was carried out by applying the following theoretical formulas (Dehnavi, et al., 2023):

Differential equation for the blade skeleton in plan:

$$d\theta = \frac{dr}{r tg\beta}; \tag{1}$$

where θ – the angle of coverage of the blade of the impeller; r – radius vector; β – the installation angle of the impeller blade.

At the same time, the angle of coverage of the blade in the plan can be expressed by the following dependence:

$$\theta = \frac{180}{\pi}\int_{r_1}^{r_2}\frac{dr}{r tg\beta}; \tag{2}$$

where r_1, r_2 radius of inlet and outlet of the impeller, respectively.

The angle of installation of the blade at any radius can be determined according to the dependence:

$$\sin\beta = \frac{S}{l} + \frac{V_m`}{W} \tag{3}$$

where S – blade thickness, l – blade length, V_m – meridional component of absolute velocity, W – relative velocity.

The subject of analysis is the operating process in the flowing part of the TFP 125-50 pump equipped with a standard impeller and an impeller with two missing blades.

To solve this problem, an impeller design with two missing blades was used. Compared to the standard variant, the proposed configuration has 6 blades instead of 8. The calculation was performed both for the standard impeller (Fig. 2a) and for the variant with omitted blades (Fig. 2b).

The three-dimensional model of the liquid in the flowing part of the pump body (Fig. 3) remains the same for both versions of the impellers and was created using the Solidworks software.

The three-dimensional model of the liquid in the inter-blade channels of the impeller is presented for the standard impeller (Fig. 4 a) and for the proposed variant (Fig. 4 b).

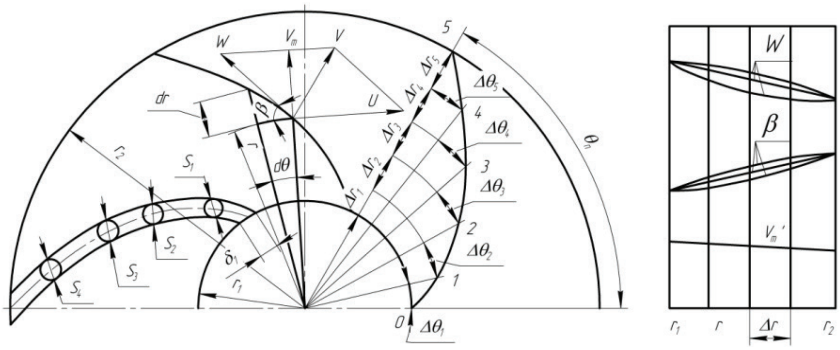

Fig. 1. The sequence of building the skeleton (design) of the impeller blade

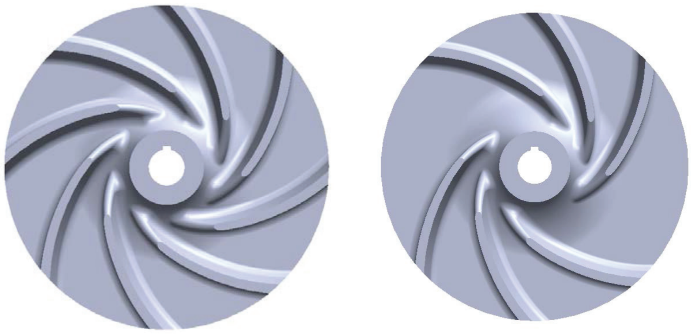

a b

Fig. 2. Three-dimensional model of the TFP 125/50 pump impeller: a – basic option; b – the proposed option

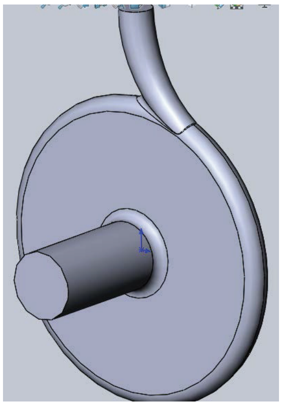

Fig. 3. Three-dimensional model of the liquid in the TFP 125/50 pump flowing part of the case

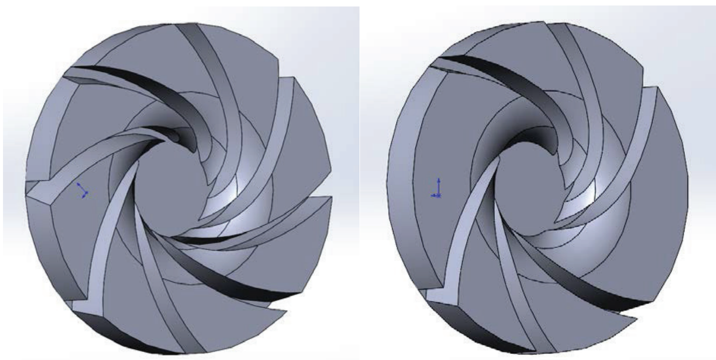

a b

Fig. 4. Three-dimensional model of the liquid in the inter-blade channels of the impeller for the standard (a) and for the proposed impeller (b)

To conduct a numerical research (Kondus, et al., 2021), a calculation grid was created using the ICEM CFD software package. The calculation area includes two main elements: the free chamber of the pump body (Fig. 5) is a stator element, and the impeller (Fig. 6) is a rotating element. An unstructured calculation grid was constructed for both of these elements.

A layer of prismatic cells was used to model the flow in the boundary layer near solid walls (Gerlach, et al., 2016). A tetrahedral mesh was used in the central part of the flow, both in the free chamber and for the impeller. The total number of elements of the calculation grid was 1 million 550 thousand cells. Flow modeling was performed in a stationary setting.

The computational model was created in the Ansys CFX environment. Water at a temperature of 25ºC was used as the operating environment. The operating mode was defined as turbulent. The standard k-ε turbulence model was used to solve the Reynolds equations. This model makes it possible to describe the turbulent movement of fluid in the flow part of the TFP torque-flow pump with sufficient accuracy up to 5% (Dehnavi, et al., 2024).

As a boundary condition at the entrance to the calculation area, the mass flow through one channel of the impeller was set, which was determined using the appropriate formula:

$$G = Q \cdot \rho; \tag{4}$$

where ρ is the density of the operating environment, Q is the volume flow rate of liquid passing through the flow part of the pump.

The boundary condition at the outlet of the computational domain was defined as a static pressure fixed at 1 MPa, since all further studies and comparisons were made for relative values. Given the possibility of reverse flows at the exit from the calculation area, the type of boundary condition was set as "opening", which allows free movement of fluid in both directions. The convergence criterion was to achieve an accuracy of 10^{-4}, which is sufficient for scientific calculations (Zhang, et al., 2022).

As a result of the numerical research, data were obtained for feeds of $0.6Q_{BEP}$, $0.8Q_{BEP}$ and $1.2Q_{BEP}$ for an impeller of a conventional design and an impeller with two missing blades.

The study also presents comparative visualizations of the flow in the flow part of the pump for both variants of impellers, namely the standard impeller and the impeller with two missing blades.

Results. The obtained results are well visualized using the distribution of relative velocities in the inter-blade channels of a standard impeller and an impeller with a non-cyclic arrangement of blades near the edge of the blades, in the middle of the inter-blade channel and near the pump impeller disk.

The distribution of relative velocities in the interblade channels of the impeller at 80% of the optimal supply ($Q=0.8\ Q_{BEP}$) near the edge, in the in the middle of the inter-blade channel, and near the disc is shown in Figures 7–9.

The distribution of relative velocities in the interblade channels of the impeller at 80% of the optimal supply ($Q=0.6\ Q_{BEP}$) near the edge, in the in the middle of the inter-blade channel, and near the disc is shown in Figures 10–12.

The distribution of relative velocities in the interblade channels of the impeller at 80% of the optimal supply ($Q=1.2\ Q_{BEP}$) near the edge, in the in the middle of the inter-blade channel, and near the disc is shown in Figures 13–15.

Discussion. When looking at the patterns of relative speed distribution, the following can be noted: when using a standard impeller (fig. 7a – 14 a), a stable pattern of relative speed distribution is observed in each of the inter-blade channels. In turn, when using an impeller ((fig. 7b – 14 b) with a non-cyclic arrangement of blades (with missing blades), there is an increase in speed near the working side of the blade in the expanded inter-blade channel, an uneven distribution

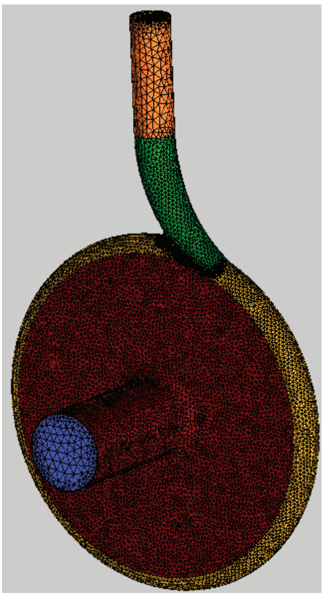

Fig. 5. Calculation grid for the flowing part of the TFP 125-50 casing

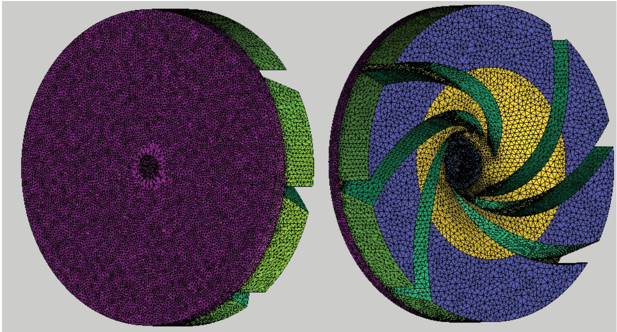

a b

Fig. 6. Calculation grid for the impeller: a – basic version; b – the proposed version

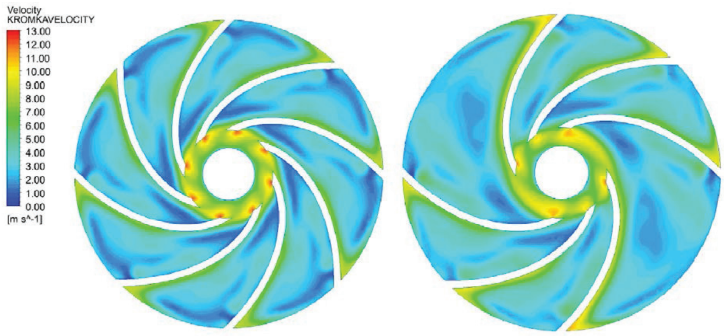

a b

Fig. 7. Distribution of relative velocity (Q=0.8 Q_{BEP}) near the edge of the blades for: a – standard impeller; b – impeller with a non-cyclic arrangement of blades

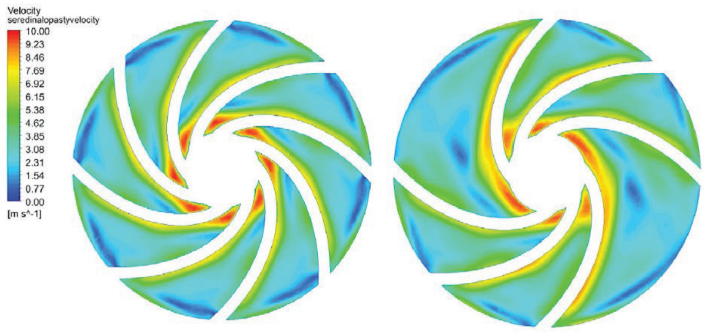

a b

Fig. 8. Distribution of relative velocity (Q=0.8 Q_{BEP}) in the middle of the inter-blade channel for: a – standard impeller; b – impeller with a non-cyclic arrangement of blades

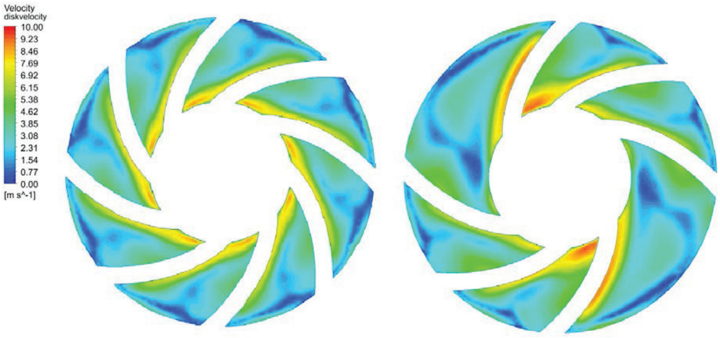

a b

Fig. 9. Distribution of relative velocity (Q=0.8 Q_{BEP}) near the pump impeller disk for: a – standard impeller; b – impeller with a non-cyclic arrangement of blades

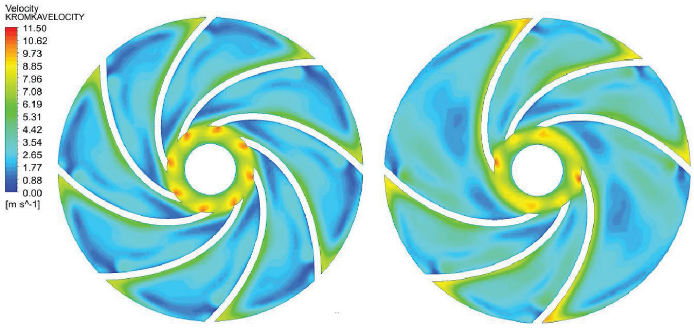

a b

Fig. 10. Distribution of relative velocity (Q=0.6 Q_{BEP}) near the edge of the blades for: a – standard impeller; b – impeller with a non-cyclic arrangement of blades

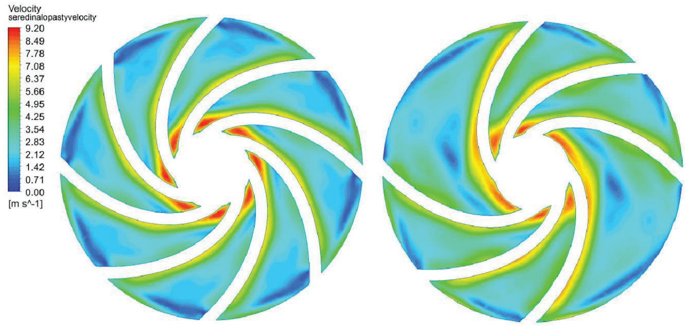

a b

Fig. 11. Distribution of relative velocity (Q=0.6 Q_{BEP}) in the middle of the inter-blade channel for: a – standard impeller; b – impeller with a non-cyclic arrangement of blades

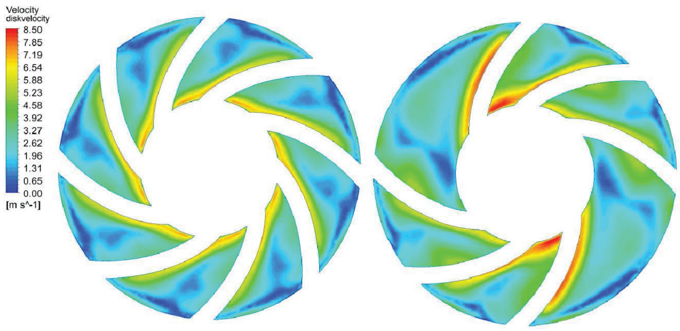

a b

Fig. 12. Distribution of relative velocity (Q=0.6 Q_{BEP}) near the pump impeller disk for: a – standard impeller; b – impeller with a non-cyclic arrangement of blades

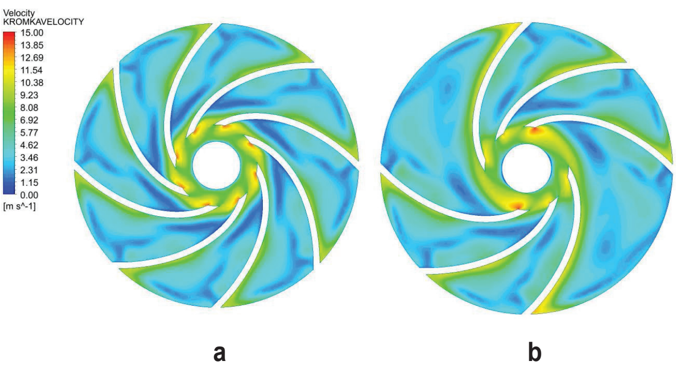

a b

Fig. 13. Distribution of relative velocity (Q=1.2 Q_{BEP}) near the edge of the blades for: a – standard impeller; b – impeller with a non-cyclic arrangement of blades

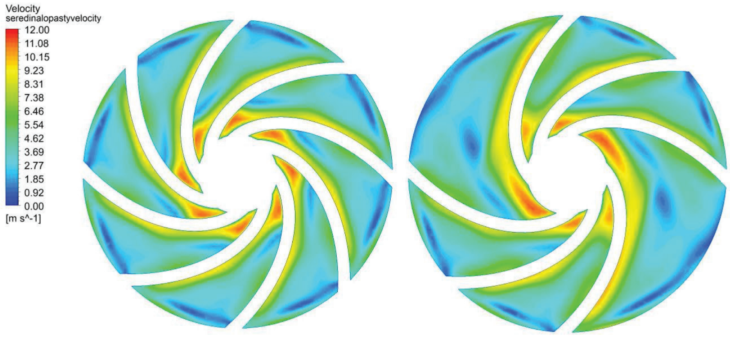

a b

Fig. 14. Distribution of relative velocity (Q=1.2 Q_{BEP}) in the middle of the inter-blade channel for: a – standard impeller; b – impeller with a non-cyclic arrangement of blades

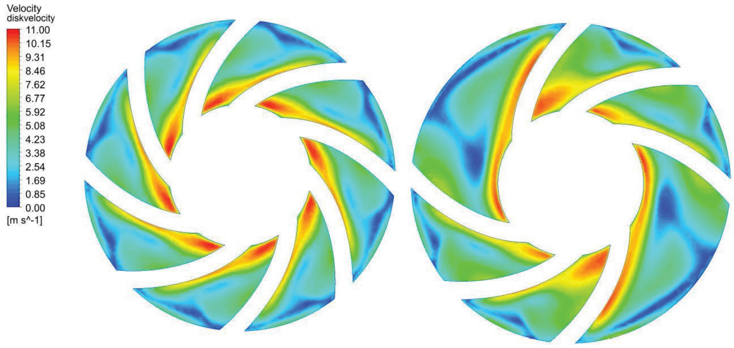

a b

Fig. 15. Distribution of relative velocity (Q=1.2 Q_{BEP}) near the pump impeller disk for: a – standard impeller; b – impeller with a non-cyclic arrangement of blades

of speed at the entrance to the wheel at the same time as the appearance of a flow separation zone in the inter-blade channels. This leads to an increase in losses, a decrease in pressure and, accordingly, the efficiency of the pump. There is a general decrease in speed from the edges to the disk.

At the same time, the above allows us to state that, according to Bernoulli's law, there is some increased pressure in the zones of reduced speed in the expanded channels of the impeller with a non-cyclic arrangement of the blades. It is this increased pressure that creates the prerequisites for unstable relative movement of the operating fluid in comparison with the use of a standard impeller. In turn, this mechanism can be used as a self-cleaning mechanism for torque-flow pumps.

Conclusions. This publication proves the perspective of using impellers with a non-cyclic arrangement of blades for the purpose of forming a self-cleaning mechanism of torque-flow pumps. When using a standard impeller, a stable relative speed distribution is observed in the inter-blade channels. A non-cyclic blade arrangement (with missing blades) causes speed increases near the blade's working side in expanded channels. This configuration results in uneven speed distribution at the wheel entrance and the formation of flow separation zones. Such phenomena lead to higher losses, reduced pressure, and lower pump efficiency. A general velecity decrease is observed from the channel edges toward the disk. According to Bernoulli's law, zones of reduced velocities in expanded channels exhibit increased pressure. This pressure contributes to unstable relative fluid movement compared to standard impeller designs. The observed mechanism can be potentially utilized as a self-cleaning feature in torque-flow pumps.

References:

1. Panchenko, V., German, V., Ivchenko, O., Ryasnaya, O. (2021). Combined operating process of torque flow pump. Journal of Physics: Conference series, Vol. 1741 012011. https://doi.org/10.1088/1742-6596/1741/1/012022

2. Gao, X., Shi, W., Zhang, D., Zhang, Q. & Fang, B. (2014). Optimization design and test of vortex pump based on CFD orthogonal test. Nongye Jixie Xuebao/Transactions of the Chinese Society for Agricultural Machinery, 45 (5), 101–106. http://dx.doi.org/10.6041/j.issn.1000-1298.2014.05.016

3. Quan, H., Chai, Y., Li, R., Guo, J. (2019). Numerical simulation and experiment for study on internal flow pattern of vortex pump. Engineering Computations, 36, 1579–1596. https://doi.org/10.1108/EC-09-2018-0420

4. Antonenko, S., Sapozhnikov, S., Kondus, V., Chernobrova, A., Mandryka, A. (2021). Creation a universal technique of predicting performance curves for small-sized centrifugal stages of well oil pump units. Journal of Physics: Conference series, Vol. 1741 012011. https://doi.org/10.1088/1742-6596/1741/1/012011

5. Gusak, O., Krishtop, I., German, V., Baga, V. (2017). Increase of economy of torque flow pump with high specific speed. IOP Conf. Ser.: Mater. Sci. Eng., 233 012004. https://doi.org/10.1088/1757-899X/233/1/012004
6. Krishtop, I. (2015). Creating the flowing part of the high energy-efficiency torque flow pump. Eastern-European Journal of Enterprise Technologies, 2 (74), 31–37. https://doi.org/10.15587/1729-4061.2015.39934
7. Kotenko, A., Herman, V., Kotenko, A. (2014). Rationalization of Ukrainian industrial enterprises in a context of using torque flow pumps on the basis of valuation of the life cycle of pumping equipment. Nauka i Studia, Vol. 16 (126), pp. 83–91. http://essuir.sumdu.edu.ua/bitstream/123456789/38769/3/kotenko_poland1.PDF
8. Kondus, V., Kalinichenko, P., Gusak, O. (2018). A method of designing of torque-flow pump impeller with curvilinear blade profile. Eastern-European Journal of Enterprise Technologies, 3/8 (93), 29–35. https://doi.org/10.15587/1729-4061.2018.131159
9. Kumar, J., Gopi, S., Amirthagadeswaran, K. (2023). Redesigning and numerical simulation of gating system to reduce cold shut defect in submersible pump part castings. Proceedings of the Institution of Mechanical Engineers, Part E: Journal of Process Mechanical Engineering, Vol. 237 (3), pp. 971-981. https://doi.org/10.1177/09544089221142185
10. Kondus, V.; Kotenko A. (2017). Investigation of the impact of the geometric dimensions of the impeller on the torque flow pump characteristics. Eastern-European Journal of Enterprise Technologies, Vol. 1/4 (88), pp. 25–31. https://doi.org/10.15587/1729-4061.2017.107112
11. Krishtop, I., German, V., Gusak, A., Lugova, S., & Kochevsky, A. (2014). Numerical Approach for Simulation of Fluid Flow in Torque Flow Pumps. In Applied Mechanics and Materials. Trans Tech Publications, Ltd., 630, 43–51. https://doi.org/10.4028/www.scientific.net/amm.630.43
12. Rogovyi, A., Korohodskyi, V., Neskorozhenyi, A., Hrechka, I., Khovanskyi, S., Reduction of Granular Material Losses in a Vortex Chamber Supercharger Drainage Channel. Advances in Design, Simulation and Manufacturing V. DSMIE 2022. Lecture Notes in Mechanical Engineering, pp. 218–226. https://doi.org/10.1007/978-3-031-06044-1_21
13. Dehnavi, E., Solis, M., Danlos, A., Kebdani, M., Bakir, F. (2023). Improving the Performance of an Innovative Centrifugal Pump through the Independent Rotation of an Inducer and Centrifugal Impeller Speeds. Energies, 16(17), 6321. https://doi.org/10.3390/en16176321
14. Jung, D.-W., Seo, C.-W., Lim, Y.-C., ... Lee, S.-Y., Suh, H.-K. (2023). Analysis of Flow Characteristics of a Debris Filter in a Condenser Tube Cleaning System. Energies, 2023, 16(11), 4472. https://doi.org/10.3390/en16114472
15. Dehghan, A., Shojaeefard, M., Roshanaei, M. (2024) Exploring a new criterion to determine the onset of cavitation in centrifugal pumps from energy-saving standpoint; experimental and numerical investigation. Energies, Vol. 293, 130681. Retrieved from http://dx.doi.org/10.1016/j.energy.2024.130681
16. Kondus V., Ciszak O., Zhukov A., Mushtai M., Polkovnychenko V., Krugliak A. (2024). Development of a self-cleaning mechanism for torque-flow pumps. Journal of Engineering Sciences, Vol. 11(2), pp. F17–F26. https://doi.org/10.21272/jes.2024.11(2).f3
17. Dehnavi, E., Bakir, F., Danlos, A., Kebdani, M. (2023). Numerical Analysis of Distance Effect between Inducer and Centrifugal Impeller in Independent Rotational Turbopump in Co-rotating and Counter-rotating Mode. European Conference on Turbomachinery Fluid Dynamics and Thermodynamics, ETC, 2023. http://dx.doi.org/10.29008/ETC2023-203
18. Kondus, V., Puzik, R., German, V., Panchenko, V., Yakhnenko, S. (2021). Improving the efficiency of the operating process of high specific speed torque-flow pumps by upgrading the flowing part design. Journal of Process Mechanical Engineering, Vol. 237, pp. 1741 012023. https://doi.org/10.1088/1742-6596/1741/1/012023
19. Gerlach, A., Thamsen, P. & Lykholt-Ustrup, F. (2016). Experimental Investigation on the Performance of a Vortex Pump using Winglets. ISROMAC 2016. International Symposium on Transport Phenomena and Dynamics of Rotating Machinery. http://isromac-isimet.univ-lille1.fr/upload_dir/finalpaper/181.finalpaper.pdf
20. Dehnavi, E., Danlos, A., Solis, M., Kebdani, M., Bakir, F. (2024). Study on the pump cavitation characteristic through novel independent rotation of inducer and centrifugal impeller in co-rotation and counter-rotation modes. Physics of Fluids, Vol. 36(1), pp. 015120. http://dx.doi.org/10.1063/5.0182731
21. Zhang, H., Deng, C., Chang, C., You, H. (2022). Novel dual synergistic sealing ring design for a high-pressure pump – Part I. http://dx.doi.org/10.12968/s1350-4789(22)70085-2
22. Zhang, H., Deng, C., Chang, C., You, H. (2022). Novel dual synergistic sealing ring design for a high-pressure pump – Part II. https://doi.org/10.12968/S1350-4789(22)70086-4

Кондусь В. Ю., *кандидат технічних наук, доцент, Сумський державний університет, м. Суми, Україна*
Кругляк А. А., *аспірант, Сумський державний університет, м. Суми, Україна*
Бага В. М., *кандидат технічних наук, доцент, Сумський державний університет, м. Суми, Україна*
Думанчук М. Ю., *кандидат технічних наук, доцент, Сумський національний аграрний університет, м. Суми, Україна*

Дослідження робочого процесу роботи вільновихрового насоса з нециклічним робочим колесом у робочому діапазоні

Вільновихрові (TFP) насоси широко застосовуються в різних галузях промисловості для перекачування забруднених, волокнистих або газовмістних рідин завдяки їх простій конструкції, надійності та низькому ризику засмічення, незважаючи на обмеження ефективності та напору. Основними недоліками вільновихрових насосів є низька енергоефективність (ККД насоса η=0,38-0,58) і можливість засмічення їх проточної частини продуктом, що перекачується. Зазначена проблема може бути вирішена шляхом забезпечення ефекту самоочищення вільновихрового насоса за допомогою проєктування робочого колеса з нерівномірним розташуванням лопатей, яке забезпечить пульсаційний характер тиску в його міжлопатевих каналах. Метою дослідження було встановлення *характеристик насоса з нерівномірно розташованими лопатями та порівняння отриманих результатів із характеристиками аналогічного насоса з рівномірно розташованими лопатями. Для проведення чисельного дослідження у програмному пакеті ICEM CFD були створені неструктуровані розрахункові сітки статорного елементу (корпус) та роторного елементу (робоче колесо). Моделювання робочого процесу насоса виконувалося у стаціонарній постановці з використанням програмного комплексу Ansys CFX, причому була використана k-ε модель турбулентності у стаціонарній постановці, в якості робочого середовища використовувалася вода за температури 25°C. За результатами дослідження встановлено, що при використанні робочого колеса з нециклічним розташуванням лопатей (з відсутніми лопатями) відбувається збільшення відносної швидкості біля робочої сторони лопаті в розширеному міжлопатевому каналі, нерівномірний розподіл швидкості на вході в колесо одночасно з появою зони відриву потоку в міжлопатевих каналах, що призводить до збільшення втрат, зменшення тиску і, відповідно, ККД насоса. У той же час вищевикладене дозволяє стверджувати, що згідно із законом Бернуллі в розширених каналах робочого колеса з нециклічним розташуванням лопатей в зонах зниженої швидкості існує деякий підвищений тиск. Саме такий підвищений тиск створює передумови для нестійкого відносного руху робочої рідини в порівнянні з використанням стандартного робочого колеса. У свою чергу, цей механізм може бути використаний як механізм самоочищення для вільновихрових насосів.*

Ключові слова: *ЦСР ООН, вібраційна надійність, вартість життєвого циклу, енергоефективність, довговічність, ефект самоочищення в насосах.*